

# Artificial Transfer Hydrogenases for the Enantioselective Reduction of Cyclic Imines\*\*

Marc Dürrenberger, Tillmann Heinisch, Yvonne M. Wilson, Thibaud Rossel, Elisa Nogueira, Livia Knörr, Annette Mutschler, Karoline Kersten, Malcolm Jeremy Zimbron, Julien Pierron, Tilman Schirmer, and Thomas R. Ward\*

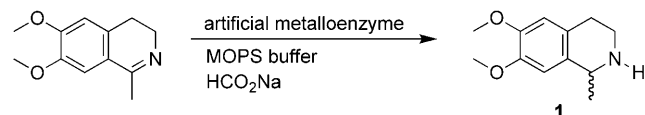
Enantiopure amines are privileged compounds which find wide use in the pharmaceutical, agrochemical, and flavor and fragrance industries. In this context, enzymatic,<sup>[1]</sup> homogeneous,<sup>[2]</sup> and chemoenzymatic<sup>[3]</sup> approaches offer complementary means for the preparation of these targets.

The asymmetric transfer hydrogenation (ATH) of ketones using d<sup>6</sup> piano stool complexes as catalyst has been the subject of numerous studies,<sup>[4]</sup> leading to a unified picture of the reaction mechanism.<sup>[5]</sup> The ATH of imines, however, has received less attention.<sup>[6]</sup> Interestingly, the reaction proceeds through a different enantioselection mechanism: for a given aminosulfonamide ligand configuration, the opposite enantiomers (alcohol vs amine) are produced.<sup>[7]</sup> In addition, it has been argued that the imine must be protonated for the reaction to proceed.<sup>[8]</sup>

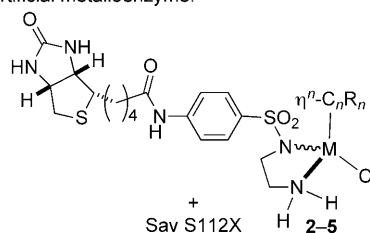
In recent years, artificial metalloenzymes, resulting from the introduction of a catalyst within a protein environment, have attracted attention as potential alternatives to traditional catalysts.<sup>[9]</sup> Based on our experience in artificial ATHs for the reduction of ketones,<sup>[10]</sup> we set out to test these systems toward the enantioselective reduction of imines and to compare their salient features with related homogeneous systems.

As a starting point, we screened d<sup>5</sup> and d<sup>6</sup> piano stool complexes bearing the biotinylated aminosulfonamide ligand (abbreviated Biot-*p*-L) combined with wild-type streptavidin (Sav) for the production of salsolidine **1** (Scheme 1).<sup>[11]</sup>

This screening led to the identification of [Cp\*Ir(Biot-*p*-L)Cl] (**5**⊂Sav) as the most promising catalyst. This contrasts with ATH of ketones for which [(η<sup>6</sup>-arene)Ru(Biot-*p*-L)Cl] **2** and **3** proved superior (Table 1).<sup>[12]</sup> In all but one case, both amine **1** and 1-phenylethanol **6** were produced with the same configuration for a given artificial metalloenzyme.



artificial metalloenzyme:



M	η <sup>n</sup> -C <sub>n</sub> R <sub>n</sub>	Abbreviation
Ru	η <sup>6</sup> - <i>p</i> -cymene	[( <i>p</i> -cymene)Ru(Biot- <i>p</i> -L)Cl] <b>2</b>
Ru	η <sup>6</sup> -benzene	[(benzene)Ru(Biot- <i>p</i> -L)Cl] <b>3</b>
Rh	η <sup>5</sup> -C <sub>5</sub> Me <sub>5</sub>	[Cp*Rh(Biot- <i>p</i> -L)Cl] <b>4</b>
Ir	η <sup>5</sup> -C <sub>5</sub> Me <sub>5</sub>	[Cp*Ir(Biot- <i>p</i> -L)Cl] <b>5</b>

**Scheme 1.** Artificial metalloenzymes based on the biotin-streptavidin technology for the ATH of imines. MOPS = 3-morpholinopropanesulfonic acid.

Next, we screened complex **5** with the saturation mutagenesis library S112X (Table 2 and Supporting Information, Table S1). Noteworthy features include:

- 1) Incorporation of [Cp\*Ir(Biot-*p*-L)Cl] (**5**) into Sav S112X produces predominantly (*R*)-**1**.
- 2) The best (*R*)-selectivities are obtained for the smallest amino acids at position 112 (S112G, S112A). The optimal pH is 6.50, affording the product in 85% *ee* at 55 °C (Table 2, entries 3 and 14).
- 3) The active biotinylated catalyst resides in the biotin-binding vestibule: addition of four equivalents of biotin to

[\*] M. Dürrenberger,<sup>[a]</sup> T. Heinisch,<sup>[a]</sup> Y. M. Wilson,<sup>[a]</sup> T. Rossel, E. Nogueira, L. Knörr, A. Mutschler, K. Kersten, M. J. Zimbron, J. Pierron, T. Schirmer, Prof. Dr. T. R. Ward  
Institut für Anorganische Chemie, Universität Basel  
Spitalstrasse 51, 4056 Basel (Switzerland)  
Fax: (+41) 61-267-1005  
E-mail: thomas.ward@unibas.ch

[†] These authors contributed equally to this work.

[\*\*] This research was supported by the Swiss National Science Foundation (Grant 200020-126366), the Cantons of Basel, and Marie Curie Training Networks (FP7-ITN-238531, FP7-ITN-238434). We thank Prof. C. R. Cantor for the Sav gene.

Supporting information for this article is available on the WWW under <http://dx.doi.org/10.1002/ange.201007820>.

**Table 1:** Results for the chemical optimization of artificial transfer hydrogenases.

Entry	Complex	<i>ee</i> [%] [conv.] <b>1</b> <sup>[a]</sup>	<i>ee</i> [%] [conv.] <b>6</b> <sup>[b]</sup>
1	<b>2</b>	22 ( <i>R</i> ) [97]	70 ( <i>R</i> ) [84]
2	<b>3</b>	12 ( <i>R</i> ) [76]	45 ( <i>S</i> ) [56]
3	<b>4</b>	52 ( <i>R</i> ) [94]	15 ( <i>R</i> ) [26]
4	<b>5</b>	57 ( <i>R</i> ) [quant.]	13 ( <i>R</i> ) [47]

[a] The reaction was carried out at 55 °C for 15 h using 1 mol% complex **2–5** (690 μM final concentration) and 0.33 mol% tetrameric WT Sav at pH 8.0 (MOPS buffer 2.9 M) containing 3.65 M HCO<sub>2</sub>Na (see Supporting Information for experimental details). [b] Data from Ref. [12].

**Table 2:** Selected results for the genetic optimization of artificial transfer hydrogenases for the production of Salsolidine **1**.<sup>[a]</sup>

Entry	Sav mutant	T [°C]	t [h]	pH	Conv. [%]	ee [%]
1	no prot.	25	5	7.25	quant.	rac.
2	WT Sav	55	2	7.25	quant.	57 (R)
3	S112G	55	2	7.25	quant.	60 (R)
4	S112R	55	2	7.25	quant.	19 (S)
5	S112K	55	2	7.50	94	35 (S)
6	S112K	55	64	7.25	30 <sup>[b]</sup>	6 (S)
7	S112K	5	48	7.50	quant.	78 (S)
8	S112K	25	24	7.25	39 <sup>[c]</sup>	44 (S)
9	S112K <sup>[d]</sup>	25	24	7.25	30 <sup>[c]</sup>	42 (S)
10	empty plasmid	25	24	7.25	43 <sup>[c]</sup>	1 (S)
11	S112A	55	2	7.25	quant.	79 (R)
12	S112A	55	64	7.25	69 <sup>[b]</sup>	27 (R)
13	S112A	55	2	7.25	59 <sup>[e]</sup>	14 (R)
14	S112A	55	2	6.50	quant.	85 (R)
15	S112A	5	24	6.50	quant.	91 (R)
16	S112A	5	24	6.50	quant. <sup>[f]</sup>	93 (R)
17	S112A	5	24	6.50	quant. <sup>[g]</sup>	88 (R)
18	S112A	5	96	6.50	quant. <sup>[h]</sup>	96 (R)
19	S112A	5	115	6.50	86 <sup>[h,i]</sup>	96 (R)
20	S112A	25	24	7.25	77 <sup>[j]</sup>	64 (R)
21	S112A <sup>[d]</sup>	25	24	7.25	65 <sup>[j]</sup>	61 (R)
22	H87A	55	2	7.25	quant.	48 (R)
23	H127A	55	2	7.25	quant.	54 (R)
24	S112AK121T	5	24	6.50	90	54 (R)

[a] See Table 1 and Supporting Information for full experimental details; S112P was expressed as inclusion bodies and thus was not tested. [b] Acetophenone reduction yielding 1-phenylethanol **6**. [c] 50  $\mu\text{M}$   $[\text{Cp}^*\text{Ir}(\text{Biot-}p\text{-L})\text{Cl}]$  (**5**; i.e. 1 mol% vs **1**) and 25  $\mu\text{M}$  S112K (tetramer). [d] Precipitated protein from cell free extracts (Supporting Information). [e] Four equivalents (vs tetrameric Sav) biotin added. [f] 0.25 mol% complex **5** and 0.25 mol% S112A tetramer. [g] 1 mol% complex **5** and 0.25 mol% S112A tetramer. [h] 0.025 mol% complex **5** and 0.025 mol% S112A tetramer. [i] 86% yield of isolated product on 100 mg scale. [j] 39  $\mu\text{M}$   $[\text{Cp}^*\text{Ir}(\text{Biot-}p\text{-L})\text{Cl}]$  (**5**; i.e. 1 mol% vs **1**) and 20  $\mu\text{M}$  S112A (tetramer).

$[\text{Cp}^*\text{Ir}(\text{Biot-}p\text{-L})\text{Cl}]\subset\text{S112A}$  affords (*R*)-**1** in low *ee* (Table 2, entry 13).

- 4) (*S*)-selectivities result from the presence of a cationic residue at position S112 (e.g. S112K and S112R, Table 2, entries 4 and 5).
- 5) Decreasing the temperature to 5 °C allows improvement of the enantioselectivity to 91% (*R*) for **5** $\subset$ S112A and 78% (*S*) for **5** $\subset$ S112K (Table 2, entries 7 and 15). Importantly, these reactions are not sensitive to traces of oxygen: no degassing is required prior to catalysis.
- 6) Up to 4000 turnovers can be achieved with no erosion of selectivity (Table 2, entry 18). On a preparative scale (100 mg substrate, 0.025 mol% catalyst), the *ee* could be further increased to 96%, with an isolated yield of 86% (Table 2, entry 19).
- 7)  $[\text{Cp}^*\text{Ir}(\text{Biot-}p\text{-L})\text{Cl}]\subset\text{S112A}$  produces the same preferred enantiomer for alcohol (*R*)-**6** and amine (*R*)-**1**. Similarly,  $[\text{Cp}^*\text{Ir}(\text{Biot-}p\text{-L})\text{Cl}]\subset\text{S112K}$  affords (*S*)-**6** and amine (*S*)-**1**, respectively (Table 2, entries 6 and 12). This suggests that both imine and ketone reduction proceed through the same enantioselection mechanism. We thus conclude that the second coordination sphere interactions provided by

the host protein outweigh the preference of the related homogeneous catalyst.

- 8) Increasing the ratio of  $[\text{Cp}^*\text{Ir}(\text{Biot-}p\text{-L})\text{Cl}]$  vs Sav tetramer from one to four leads to a gradual erosion of enantioselectivity (93 to 88% *ee*, Table 2, entries 16 and 17). This suggests that an empty biotin binding site adjacent to a  $[\text{Cp}^*\text{Ir}(\text{Biot-}p\text{-L})\text{Cl}]$  moiety within Sav may be favorable for selectivity.
- 9) Performing catalysis with Sav mutants obtained from an ethanol precipitation step on a dialyzed protein extract yields results very similar to those obtained with dilute samples of pure protein for both S112K and S112A (Table 2, compare entries 8–10 and 20–21). This finding demonstrates that  $[\text{Cp}^*\text{Ir}(\text{Biot-}p\text{-L})\text{Cl}]$  (**5**) tolerates cellular components.<sup>[13]</sup> This opens fascinating perspectives for parallel screening as it significantly shortens the protein purification effort (from 12 to 3 days).

To gain structural insight into the best (*R*)-selective artificial metalloenzyme, crystals of S112A Sav were soaked with a solution containing an excess of cofactor **5**. The X-ray crystal structure was solved to 1.9 Å resolution. Strong residual density in the  $F_o - F_c$  map indicated that all biotin-binding sites are fully occupied by ligand Biot-*p*-L (Figure 1 a,

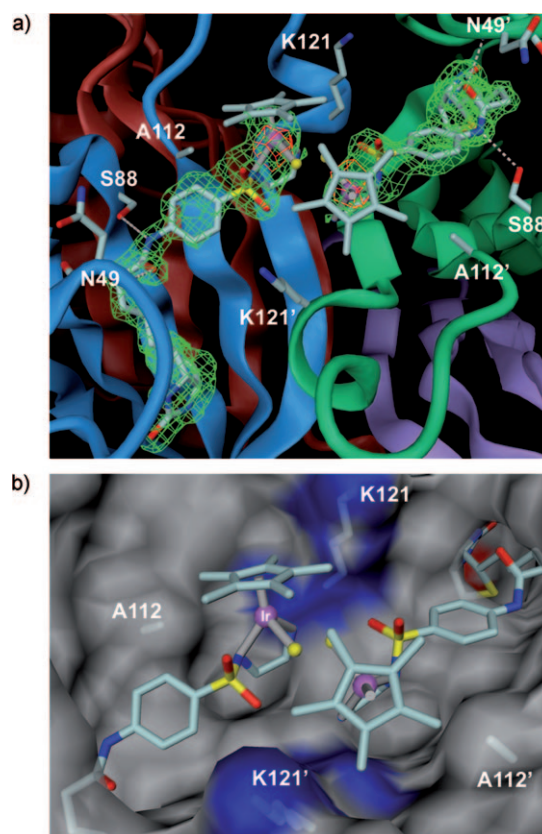


**Figure 1.** Close-up view of the X-ray crystal structure (PDB: 3pk2) of complex **5** $\subset$ S112A Sav showing two symmetry-related cofactors in the biotin-binding pocket of the protein tetramer.  $F_o - F_c$  omit map colored in green (contoured at 3  $\sigma$ ) and anomalous difference density map (5  $\sigma$ ) in red (a). Surface representation with basic residues in blue, acidic in red, polar and apolar in gray (b); (chloride: yellow sphere).

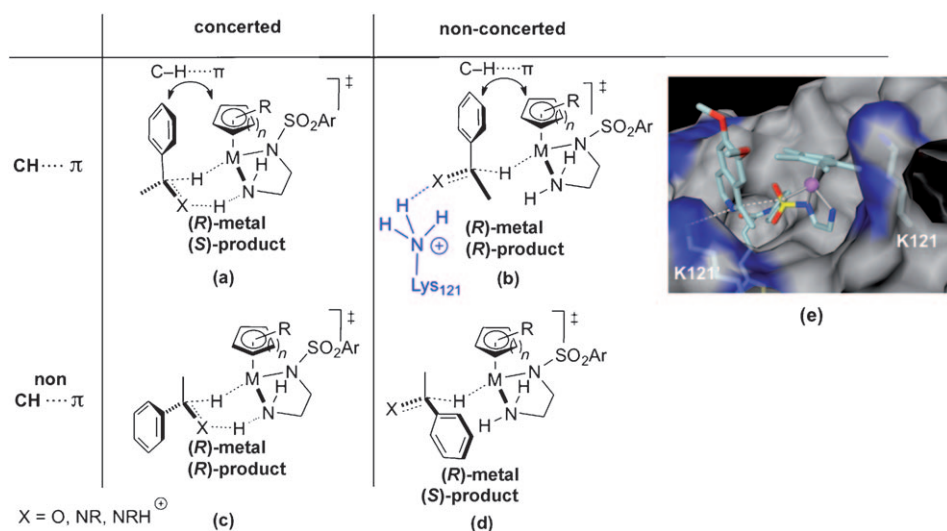


**Figure 2.** Possible transition states for the  $d^6$  piano stool catalyzed asymmetric transfer hydrogenation of ketones and imines a–d. a)  $\text{CH}\cdots\pi$  interaction combined with a contact between the imine N and K121 affords (*R*)-products (b and e; latter viewed from the empty biotin-binding pocket).

note that due to crystallographic symmetry all Sav monomers are identical). Adjacent to the ethylenediamine moiety of Biot-*p*-L a strong peak ( $15\sigma$ ) in the anomalous difference map suggested the position of iridium. To avoid negative  $F_o - F_c$  density the iridium atom occupancy was set to 50%. This most likely indicates partial dissociation of the  $\{\text{IrCp}^*\text{Cl}\}$  fragment upon soaking, since alternative conformations appear sterically not possible. The iridium atoms of two symmetry-related cofactors (face-to-face) are separated by 5.2 Å. Despite the purity of the complex used for soaking, no  $F_o - F_c$  density was found for  $\text{Cp}^*$  and chloride ligands. To prevent steric clashes between symmetry-related  $\text{Cp}^*$  groups, this bulky moiety was modeled with a dihedral angle  $\text{S-N-Ir-Cp}^*_{\text{centroid}} = 98.3^\circ$  (and  $\text{S-N-Ir-Cl} = -34.2^\circ$ ). This sets the configuration at Ir in the structure to (*S*)- $[\text{Cp}^*\text{Ir}(\text{Biot-}p\text{-L})\text{Cl}]$  (and correspondingly (*R*)- $[\text{Cp}^*\text{Ir}(\text{Biot-}p\text{-L})\text{H}]$ ).

Compared to the recently characterized  $[(\eta^6\text{-benzene})\text{Ru}(\text{Biot-}p\text{-L})\text{Cl}]$  (**3**; S112K; PDB: 2qcb, an (*S*)-selective ATH),<sup>[10]</sup> the absolute configuration at the metal is (*S*) in both cases, but the metal fragment is rotated along the aryl–S bond by about  $150^\circ$ . This prevents steric clashes between the benzene moiety and K121 of the adjacent monomer B (Figure S2b).

Additional anomalous difference density indicating iridium was found in the vicinity of the  $\text{N}_e$  atoms of H87 and H127 (Figure S2c,d). These species, however, are not involved in catalysis, as demonstrated by the results obtained with the H87A and H127A mutants which are nearly identical to those obtained with WT Sav (Table 2, entries 22 and 23).

Assuming that the absolute configuration revealed in the X-ray structure is catalytically active, two transition states leading to the observed (*R*)-products (alcohol or amine) can be envisaged: non-concerted +  $\text{CH}\cdots\pi$  or concerted + non- $\text{CH}\cdots\pi$ , respectively (Figure 2b,c). Qualitative modeling of the imine substrate into a vacated neighboring biotin site was carried out for both possible transition states leading to (*R*)-**1**. For the concerted + non- $\text{CH}\cdots\pi$  mechanism, steric clashes

between the substrate's aromatic group and the protein project the imine moiety into the  $\text{Cp}^*$  fragment (Figure S2e). In contrast, for the non-concerted +  $\text{CH}\cdots\pi$  interaction, no steric clashes with the protein are apparent (Figure 2e). Interestingly, the imine functionality lies close to the ammonium group of K121 (of the adjacent monomer). This contact may replace the amine group of the ligand for the delivery of a proton to the substrate (Figure 2b,e). To test this possibility, the double mutant S112AK121T was tested in catalysis (Table 2, entry 24). The erosion in enantioselectivity suggests that the non-concerted +  $\text{CH}\cdots\pi$  mechanism is operative both for the ATH of ketones and imines.

is operative both for the ATH of ketones and imines.

In summary, introduction of a biotinylated iridium piano stool complex  $[(\eta^5\text{-Cp}^*)\text{Ir}(\text{Biot-}p\text{-L})\text{Cl}]$  (**5**) within streptavidin affords an artificial imine reductase. Both (*R*)-**1** (96% *ee*) and (*S*)-**1** (78% *ee*) are accessible with the same organometallic moiety. This corresponds to a  $\Delta\Delta G^\ddagger$  of  $3.3 \text{ kcal mol}^{-1}$  for a single-point mutation. With the implementation of laboratory evolution protocols for the optimization of artificial metalloenzymes for the reduction of more challenging imines in mind,<sup>[1,14]</sup> we have shown that the screening can be performed in air with up to 4000 TON and, most importantly, on precipitated protein rather than on rigorously purified Sav samples used thus far. Based on X-ray structural data, we suggest that the reaction proceeds, both for the imine and the ketone reduction, through a non-concerted +  $\text{CH}\cdots\pi$  interaction,<sup>[7b,15]</sup> whereby the residue K121 may be involved in the protonation step.

Received: December 12, 2010

Published online: February 24, 2011

**Keywords:** artificial metalloenzymes · asymmetric catalysis · imine reduction · piano stool complexes · transfer hydrogenation

[1] N. J. Turner, *Nat. Chem. Biol.* **2009**, *5*, 567–573.

[2] a) T. C. Nugent, M. El-Shazly, *Adv. Synth. Catal.* **2010**, *352*, 753–819; b) N. Fleury-Brégeot, V. de La Fuente, S. Castillon, C. Claver, *ChemCatChem* **2010**, *2*, 1346–1371.

[3] L. K. Thalén, D. Zhao, J.-B. Sortais, J. Paetzold, C. Hoben, J.-E. Bäckvall, *Chem. Eur. J.* **2009**, *15*, 3403–3410.

[4] R. Noyori, S. Hashiguchi, *Acc. Chem. Res.* **1997**, *30*, 97–102.

[5] a) M. Yamakawa, I. Yamada, R. Noyori, *Angew. Chem.* **2001**, *113*, 2900–2903; *Angew. Chem. Int. Ed.* **2001**, *40*, 2818–2821; b) M. Yamakawa, I. Yamada, R. Noyori, *Angew. Chem.* **2001**, *113*, 2900–2903; c) S. E. Clapham, A. Hadzovic, R. H. Morris, *Coord. Chem. Rev.* **2004**, *248*, 2201–2237; d) T. Ikariya, A. J. Blacker, *Acc. Chem. Res.* **2007**, *40*, 1300–1308.

- [6] a) N. Uematsu, A. Fujii, S. Hashiguchi, T. Ikariya, R. Noyori, *J. Am. Chem. Soc.* **1996**, *118*, 4916–4917; b) C. Li, J. Xiao, *J. Am. Chem. Soc.* **2008**, *130*, 13208–13209; c) L. Evanno, J. Ormala, P. M. Pihko, *Chem. Eur. J.* **2009**, *15*, 12963–12967; d) C. Wang, C. Li, X. Wu, A. Pettman, J. Xiao, *Angew. Chem.* **2009**, *121*, 6646–6650; *Angew. Chem. Int. Ed.* **2009**, *48*, 6524–6528; e) C. Wang, C. Li, X. Wu, A. Pettman, J. Xiao, *Angew. Chem.* **2009**, *121*, 6646–6650; *Angew. Chem. Int. Ed.* **2009**, *48*, 6524–6528; f) J. Wu, F. Wang, Y. Ma, X. Cui, L. Cun, J. Zhu, J. Deng, B. Yu, *Chem. Commun.* **2006**, 1766–1768.
- [7] a) J. Mao, D. C. Baker, *Org. Lett.* **1999**, *1*, 841–843; b) J. E. D. Martins, G. J. Clarkson, M. Wills, *Org. Lett.* **2009**, *11*, 847–850.
- [8] a) J. B. Aberg, J. S. M. Samec, J. Bäckvall, *Chem. Commun.* **2006**, 2771–2773; b) D. G. Blackmond, M. Ropic, M. Stefinovic, *Org. Process Res. Dev.* **2006**, *10*, 457–463.
- [9] a) Y. Lu, N. Yeung, N. Sieracki, N. M. Marshall, *Nature* **2009**, *460*, 855–862; b) F. Rosati, G. Roelfes, *ChemCatChem* **2010**, *2*, 916–927; c) M. T. Reetz, *Top. Organomet. Chem.* **2009**, *25*, 63–92; d) S. Abe, T. Ueno, Y. Watanabe, *Top. Organomet. Chem.* **2009**, *25*, 25–43; e) Q. Jing, R. J. Kazlauskas, *ChemCatChem* **2010**, *2*, 953–957; f) P. J. Deuss, G. Popa, C. H. Botting, W. Laan, P. C. Kamer, *Angew. Chem.* **2010**, *122*, 5443–5445; *Angew. Chem. Int. Ed.* **2010**, *49*, 5315–5317; g) P. J. Deuss, G. Popa, C. H. Botting, W. Laan, P. C. Kamer, *Angew. Chem.* **2010**, *122*, 5443–5445; *Angew. Chem. Int. Ed.* **2010**, *49*, 5315–5317; h) J. Podtetenieff, A. Taglieber, E. Bill, E. J. Reijerse, M. T. Reetz, *Angew. Chem.* **2010**, *122*, 5277–5281; *Angew. Chem. Int. Ed.* **2010**, *49*, 5151–5155; i) J. Podtetenieff, A. Taglieber, E. Bill, E. J. Reijerse, M. T. Reetz, *Angew. Chem.* **2010**, *122*, 5277–5281; *Angew. Chem. Int. Ed.* **2010**, *49*, 5151–5155; j) T. Heinisch, T. R. Ward, *Curr. Opin. Chem. Biol.* **2010**, *14*, 184–199; k) P. Fournier, R. Fiammengo, A. Jäschke, *Angew. Chem.* **2009**, *121*, 4490–4493; *Angew. Chem. Int. Ed.* **2009**, *48*, 4426–4429; l) P. Fournier, R. Fiammengo, A. Jäschke, *Angew. Chem.* **2009**, *121*, 4490–4493; *Angew. Chem. Int. Ed.* **2009**, *48*, 4426–4429.
- [10] a) M. Creus, A. Pordea, T. Rossel, A. Sardo, C. Letondor, A. Ivanova, I. LeTrong, R. E. Stenkamp, T. R. Ward, *Angew. Chem.* **2008**, *120*, 1422–1426; *Angew. Chem. Int. Ed.* **2008**, *47*, 1400–1404; b) M. Creus, A. Pordea, T. Rossel, A. Sardo, C. Letondor, A. Ivanova, I. LeTrong, R. E. Stenkamp, T. R. Ward, *Angew. Chem.* **2008**, *120*, 1422–1426; *Angew. Chem. Int. Ed.* **2008**, *47*, 1400–1404.
- [11] T. S. Kaufman, *Tetrahedron: Asymmetry* **2004**, *15*, 1203–1237.
- [12] C. Letondor, A. Pordea, N. Humbert, A. Ivanova, S. Mazurek, M. Novic, T. R. Ward, *J. Am. Chem. Soc.* **2006**, *128*, 8320–8328.
- [13] a) C. Streu, E. Meggers, *Angew. Chem.* **2006**, *118*, 5773–5776; *Angew. Chem. Int. Ed.* **2006**, *45*, 5645–5648; b) C. Streu, E. Meggers, *Angew. Chem.* **2006**, *118*, 5773–5776; *Angew. Chem. Int. Ed.* **2006**, *45*, 5645–5648; c) V. Köhler, Y. M. Wilson, C. Lo, A. Sardo, T. R. Ward, *Curr. Opin. Biotechnol.* **2010**, *21*, 744–752.
- [14] M. T. Reetz, J. J.-P. Peyerlans, A. Maichele, Y. Fu, M. Maywald, *Chem. Commun.* **2006**, 4318–4320.
- [15] J. E. D. Martins, M. A. C. Redondo, M. Wills, *Tetrahedron: Asymmetry* **2010**, *21*, 2258–2264.